Exothermically Assisted Shielded Metal Arc Welding

Adding exothermic flux to SMAW electrodes enhances heat generation and increases melting rate

BY J. W. ALLEN, D. L. OLSON AND R. H. FROST

ABSTRACT. Exothermic flux additions to SMAW electrodes can assist in the generation of heat and increase the rate of electrode melting. The exothermic additions consisted of various combinations and concentrations of aluminum and magnesium powders in a mixture with hematite. Aluminum reactive additions were significantly more effective than magnesium-rich additions at melting the electrode, melting the weld bead and penetrating the base plate. Magnesium was less effective at supplying heat because its reaction rate was too fast with respect to the electrode melting rate. This magnesium "exothermic meltback" prevented effective transfer of the chemically generated heat to the base plate. The rate at which the exothermic reaction occurs with respect to the melting rate of the electrode determines the efficiency with which the exothermic heat is used for welding. Exothermic reactions can produce as much as 25–30% of the total heat necessary to produce a shielded metal arc weld.

Introduction

The welding arc normally supplies the energy required to fuse the base plate material and the metal transferred from the consumable electrode. The resulting heat flow determines many physical and chemical changes that occur during arc welding and is responsible for the formation of the weld deposit. This research was to determine the heating potential of exothermic additions to the flux coating of shielded metal arc welding (SMAW) consumables. Oxidation reactions of elements such as magnesium, aluminum or titanium are known to produce significant amounts of heat. It is possible that such reactions in SMAW flux coatings could assist heat generation during arc welding. Theoretical calculations indicate that with high concentrations of exothermic additions it may be possible to formulate a welding flux that can supply all or most of the heat required for welding.

An investigation of alternative heat sources must consider the total quantity of metal, both electrode and base metal, that is melted to form the weld deposit. Two weld deposit features that relate directly to the weld parameters, and thus indirectly to heat input, are the weld penetration depth and the weld cross-sectional area. Jackson and Shrubsall (Ref. 1) have studied the effect of current, voltage and travel speed on penetration for gas metal arc welds. Olson and Schwemmer (Ref. 2) suggested that there are other factors that also influence penetration, such as arc stability, slag viscosity and interfacial tension forces. A combined form of the Jackson-Shrubsall and Schwemmer equations that takes into account both welding process parameters and slag behavior has been suggested, and is given as

$$P = K'(\gamma_{fl} - \gamma_{fm})\eta\Delta V\left(\frac{I^4}{SV^2}\right)^{1/3} + C \quad (1)$$

J. W. ALLEN, D. L. OLSON and R. H. FROST are with the Center for Welding, Joining and Coatings Research, Colorado School of Mines, Golden, Col.

KEY WORDS

SMAW
Exothermic
Electrodes
Aluminum Powders
Magnesium Powders
Hematite
Melting Rate
Calorimeter

where I is current, S is travel speed, V is arc voltage, ΔV is arc instability, η is flux viscosity, γ is interfacial tensions and K' and C are constants for a given flux system (Ref. 3).

Heat input, H, is the quantity of energy introduced from the arc per unit length of weld. It is expressed in J/mm and is calculated as the ratio of the total power input (W = VI) to the travel speed of the welding arc in mm/s multiplied by a dimensionless efficiency factor, ε.

$$H = \varepsilon\frac{VI}{S} \quad (2)$$

The efficiency term, ε, compensates for losses during energy transfer from the power supply to the workpiece. A direct, linear correlation between the weld bead cross-sectional area and the heat input has been reported (Ref. 4). Theoretically, one joule of heat will melt 0.0854 mm^3 of steel, assuming the temperature of the molten steel during welding is 1750°C.

Because the weld bead is formed from both the melted base plate and the melted electrode, the effects of welding variables on electrode melting characteristics have been investigated (Refs. 5–11). It has been shown that the electrode melting rate increases with current. In fact, a number of variables have been shown to affect electrode melting rate, including current, polarity and electrode diameter. Hummitzsch (Ref. 12) investigated the effect of the ionization potential of the SMAW flux coating on the electrode melting rate. He related the heats of formation, vaporization and ionization of the compounds in the coating to the electrode melting rate. The lowest melting rates were reported for cerium and barium compounds, while higher melting rates were observed for magnesium, titanium and silicon compounds.

The addition of different compounds to a welding arc can change both its temperature and its ability to transfer heat to

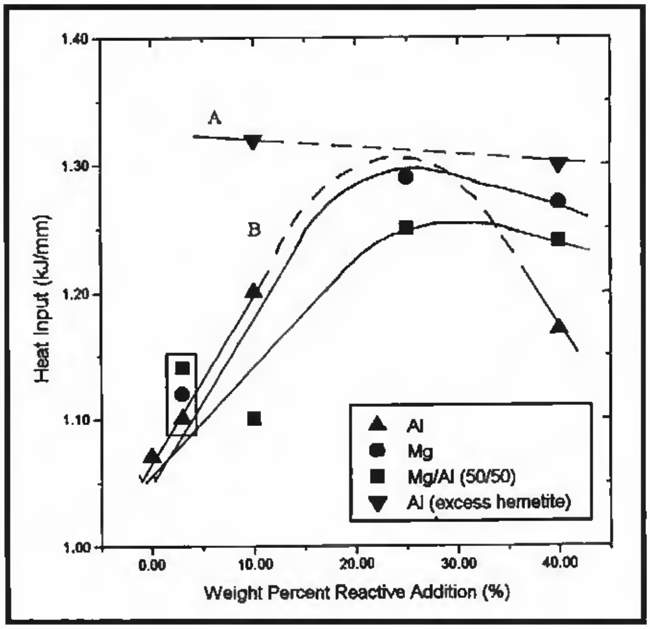

Fig. 1 — Measured heat input as a function of reactive addition. Boxed points indicate approximately equal measured heat. The effect of excess hematite on measured heat input for the aluminum-reactive electrodes can be seen by comparing line A with line B.

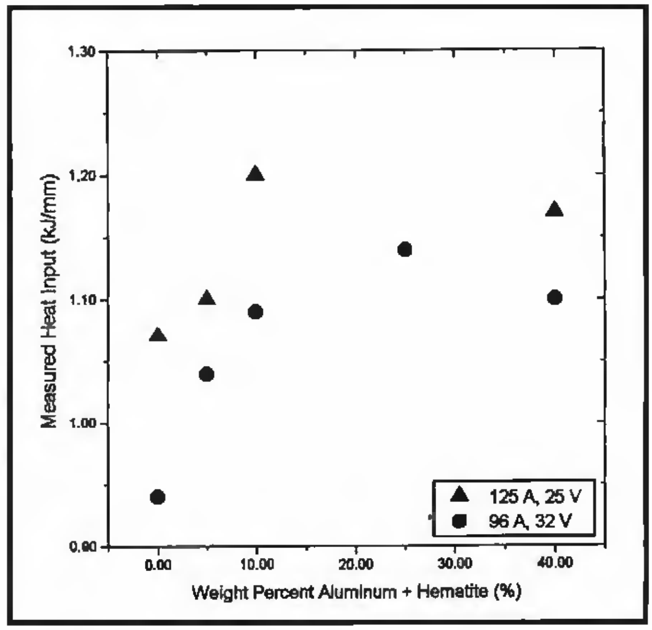

Fig. 2 — The effect of welding parameters at the same power on measured heat input of the aluminum-reactive electrodes.

the weld deposit. Flux additions that are capable of producing heat through exothermic interactions may or may not change the arc efficiency, but are potential arc heat generators. This investigation considers the potential usefulness of such exothermic flux additions and quantifies their heating and melting abilities through calorimetry.

Exothermically Assisted Welding Consumables

Exothermic welding systems are not a new concept to the welding industry. Thermite welding was developed about a century ago. Goldschmidt discovered that if finely divided metallic oxides are mixed with aluminum powder they will, if ignited, fuse and produce temperatures of 2500°C in less than 30 s (Ref. 13). The amount of heat generated during the oxidation of metals can be calculated using tabulated thermodynamic data (Ref. 14). These calculations make it possible to evaluate the potential productivity of specific chemical heat sources. Metals such as calcium, magnesium and aluminum are among the most reactive and have very large negative values for their free energies of formation (ΔG_f) and enthalpies of formation (ΔH_f). The more negative the enthalpy of formation, the more heat that is generated during the reaction. The quantities of heat produced by the reactions between aluminum with hematite and magnesium with hematite are calculated to be 566 kJ/mol O_2 and 1060 kJ/mol O_2, respectively. The most common thermite reaction is

$$2Al + Fe_2O_3 =$$
$$Al_2O_3 + 2Fe + 566\ kJ\ /\ Mol\ O_2 \quad (3)$$

Glushchenko (Ref. 15) has investigated the effects of exothermic additions in submerged arc welding fluxes on deposition rate and melting efficiency. He has derived equations that were reported to predict these behaviors for a given exothermic flux mixture. Zarechenskii (Ref. 16) has used the exothermic reaction between a magnesium/aluminum alloy and hematite to increase the melting efficiency of the flux cored arc welding process. This study indicates that the additional heat produced by the reactive addition assists in melting the flux core, which is thought to be the limiting factor to melting efficiency for flux cored arc welding.

Karpenko (Ref. 17) investigated the effects of exothermic (aluminum + iron oxide) additions on the melting characteristics of SMAW electrodes. The results of this study indicated that reactive additions increase the weld deposition rate and that there exists a particular set of welding parameters and oxide-to-reactive element ratio that optimizes productivity. Ioffe, *et al.* (Ref. 18), studied the effects of a titanothermite mixture on melting behavior and derived theoretical equations to predict the percent increase in heating due to exothermic reactions. He reported increases from 3 to 26% in heat generation and increases of 8 to 29% in melting efficiency depending upon the amount of exothermic additions in the flux coating.

These results suggest that exothermic additions could enable large SMAW electrodes to be used with small, portable, low-power electrical sources. Exothermic additions may also allow welding consumables to be used with lower welding currents, which could conceivably alleviate overheating and arc blow complications.

Preliminary Investigation

A preliminary investigation was performed that identified the effects of potential reactive additions on the welding process. The preliminary results led to the selection of the appropriate flux systems used in the primary investigation.

Table 1 — Beginning Flux Base Composition Selected for Exothermic Modification

Ingredient	Weight-Percent
Alumina	3.0
Feldspar	7.5
Calcium Carbonate	13.63
Iron-Manganese	2.46
Potassium Titanate	12.07
Rutile	51.96
Silica	9.39

The selected flux system to be investigated was initially developed by Flemming, *et al.* (Ref. 19), and has the ease of use that is characteristic of acidic SMAW fluxes, but still maintains a low weld metal oxygen content. The composition for this formulation is listed in Table 1. This flux was mixed with an aluminum + hematite (one-sixteenth of the stoichiometric ratio) mixture to form 0, 3 and 10 wt-% mixtures of reactive addition in the base flux. The fluxes were then bound with a potassium silicate binder and extruded onto a low-carbon steel core wire. The electrodes were baked at 325°C for 2 h and then used to make bead-on-plate welds on ASTM A36 steel.

The weld deposits were cut, ground, polished, photographed and measured with the image analysis system. The deposited slags and weld beads were visually examined for uniformity and porosity. Up to the 3 wt-% level, the weld bead and slag were uniform and no porosity was present in the weld deposit. The weld bead area and penetration depth were found to actually decrease with increasing exothermic reagent. At the 10-wt-% level the weld bead and slag were nonuniform and there was a drastic drop in the nugget size and the penetration. It is thought that increasing exothermic additions promoted the formation of alumina through the exothermic reaction and raised the viscosity of the molten slag. This behavior caused the irregular bead due to the lack of fluidity in the molten flux.

Based on these findings, a 20 wt-% addition of calcium fluoride was added to the base flux, giving the new composition listed in Table 2. Calcium fluoride is commonly employed to increase the fluidity of slags for steel making. It was found that the flux with the additional calcium fluoride produced a more uniform bead with a larger cross section and deeper penetration. This new base composition was then tested with a 40 wt-% addition of the exothermic reagent and was found to perform acceptably. The weld bead was uniform throughout its length and possessed consistent properties. The new base composition (Table 2) was selected to be a suitable flux for the primary investigation.

Primary Investigation

A liquid nitrogen calorimeter was used to measure the amount of heat that was transferred to the base plate when welding with exothermically assisted consumables. This technique relates the amount of liquid nitrogen vaporized by a weld specimen to its heat content (Ref. 20). The calorimeter consists of a Denver Instrument DI-8K, 8000-g-capacity balance equipped with a level-compatible RS-232C interface and a 6-L stainless steel dewar flask with lid. The dewar flask acts as a reservoir for liquid nitrogen and sets on the balance. The RS-232C interface allows weight information to be transmitted from the balance to a Fortis 386-SX personal computer. The data acquisition software for this experiment was written in Visual Basic, which permitted control of the acquisition rate and range and allowed real-time monitoring of the acquisition process.

Table 2 — Flux Base Composition Modified with Calcium Fluoride Addition

Ingredient	Weight-Percent
Alumina	2.7
Feldspar	6.7
Calcium Carbonate	12.2
Iron-Manganese	2.2
Potassium Titanate	10.8
Rutile	37
Silica	8.4
Calcium Fluoride	20.0

Initial verification and calibration of the calorimeter was accomplished by measuring the heat content of a copper test block. The test block was heated in a muffle furnace and its heat content was measured with the calorimeter at temperatures ranging from room temperature to 1173°C. Theoretical calculations of the heat content were used to verify the measurements made with the calorimeter. The calculations were based upon tabulated thermodynamic data (Ref. 14). Some manipulation of the measured heat data was required to obtain the actual heat contents of the copper test blocks. Consideration of the amount of liquid nitrogen that would boil off due to the ambient temperature in the room, the buoyant force exerted by suspending the block in the liquid nitrogen and the sensible heat of the block at room temperature was necessary.

The ambient boil-off rate (ABR) of the

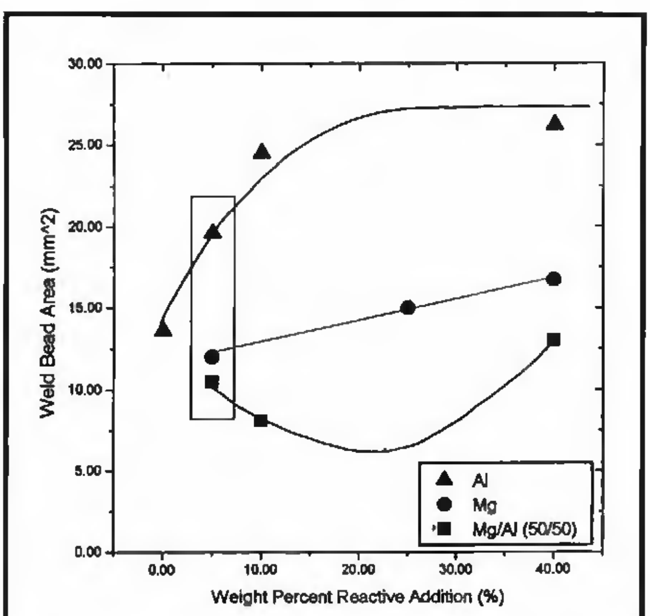

Fig. 3 — Boxed points indicate weld bead area produced with the same measured heat input.

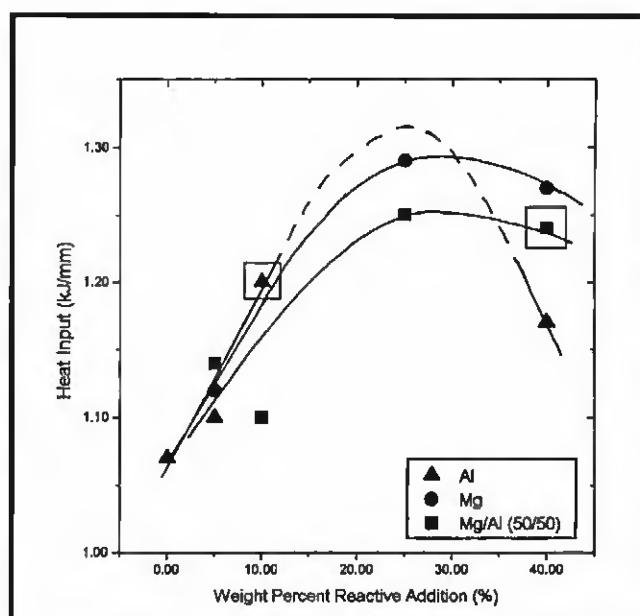

Fig. 4 — Measured heat input as a function of reactive addition. Boxed points indicate approximately equal measured heat.

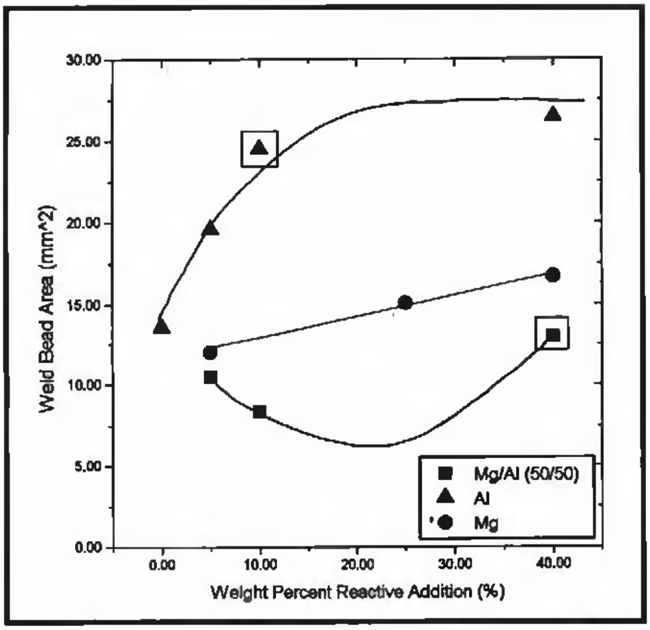

Fig. 5 — Boxed points indicate weld bead area produced with the same measured heat input.

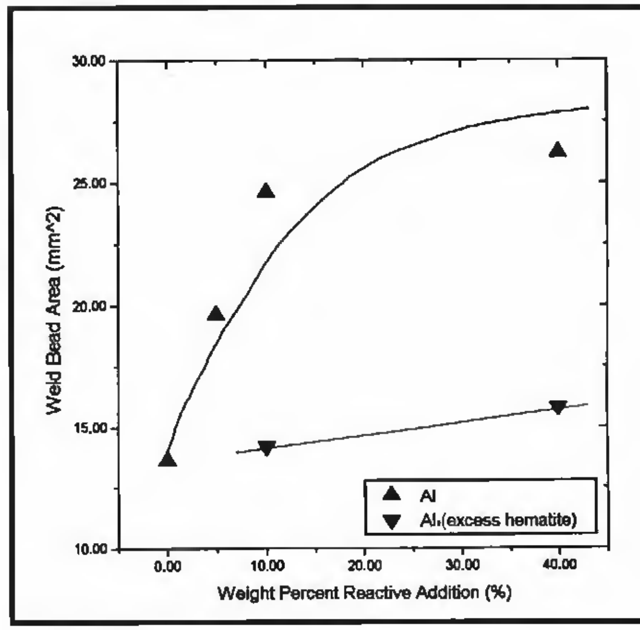

Fig. 6 — The effect of excess hematite on weld bead area.

liquid nitrogen was determined at two different temperatures, 23 and 26°C. A best fit regression line was used to determine the amount of liquid nitrogen lost during the time of the actual welding tests.

The buoyant force produced by both the copper calibration block and three different masses of steel was measured using the calorimetric apparatus and calculated using available material physical parameters. Because of the difficulty in machining test specimens of precisely the same mass (and therefore the same buoyant force and sensible heat), it was necessary to construct calibration curves that related sample mass to sensible heat and buoyant force. After determining the ABR, the buoyant force and the sensible heat of the copper test block, the calorimeter was calibrated to measure heat contents within the range of interest (20–30 kJ/mol).

A consistent overmeasurement of the heat content of the test block was observed. This overmeasurement was attributed to an additional absorption of heat by the calorimeter caused by the turbulent boiling of the liquid nitrogen on the sides and lid of the dewar.

Materials and Experimental Consumables

Fourteen electrodes were formulated with three types of exothermic reagents. Four fluxes were made with aluminum thermite, three fluxes with magnesium thermite, four fluxes with a 50/50 wt-% aluminum/magnesium alloy thermite, one flux with the pure base flux composition and two fluxes with excess hematite, which is the primary oxygen source for the reaction. The electrodes were formulated with increasing concentrations of exothermic reagents. The exothermic formulations were made by mixing a 10-kg batch of the base composition and then adding the exothermic reagents in the various weight percentages indicated in Table 3. Initially, the ratio of hematite-to-exothermic reagent was stoichiometric, but poor extrudability later required a ratio of 16% of stoichiometry.

The ingredients were dry mixed in a V-blender with ceramic grinding balls for approximately 20 min. After mixing, the ingredients were emptied into a stainless steel mixing bowl and thoroughly combined with a potassium silicate binder. The amount of binder necessary to obtain the correct consistency for extrusion varied depending upon the composition of the mixture. This dependence was primarily due to the difference in particle sizes, the smaller particles requiring more binder. In general, 1400 g of flux required between 300 and 500 g of potassium silicate binder.

The flux was extruded onto AISI-SAE 1008 steel cored wire, which had a diameter of 3.175 mm. The coating was extruded with a 5.26-mm-diameter die, giving a coating-to-wire ratio of 1.66, which is within the recommended ratios reported in the literature (Ref. 21). The electrodes were allowed to air dry for 24 h and were then baked at 325°C for 2 h.

Sixty 19.1-mm-thick ASTM A36 steel base plate specimens were cut 54 mm wide and 127 mm long. Approximately 2 ft (0.6 m) of stainless steel wire was GMA welded to one edge of each plate. The wire would later suspend the as-welded

Table 3 — Exothermic Additions to the Base Flux for the Final Test Matrix of Exothermically Assisted Welding Electrodes

	Electrode Designation and Composition (Weight-Percent)													
Ingredient	S1	A5	A10	A25	A40	M5	M25	M40	MA5	MA10	MA25	MA40	A10X	A40X
Hematite	X	1.7	3.3	8.3	13.3	0.83	1.66	6.7	1.1	2.23	5.55	8.9	6.6	26.6
Aluminum	X	3.3	6.7	16.7	26.7	X	X	X	X	X	X	X	6.7	26.6
Magnesium	X	X	X	X	X	4.16	8.33	33.3	X	X	X	X	X	X
Mg/Al Alloy (50/50)	X	X	X	X	X	X	X	X	3.4	7.77	19.45	31.1	X	X

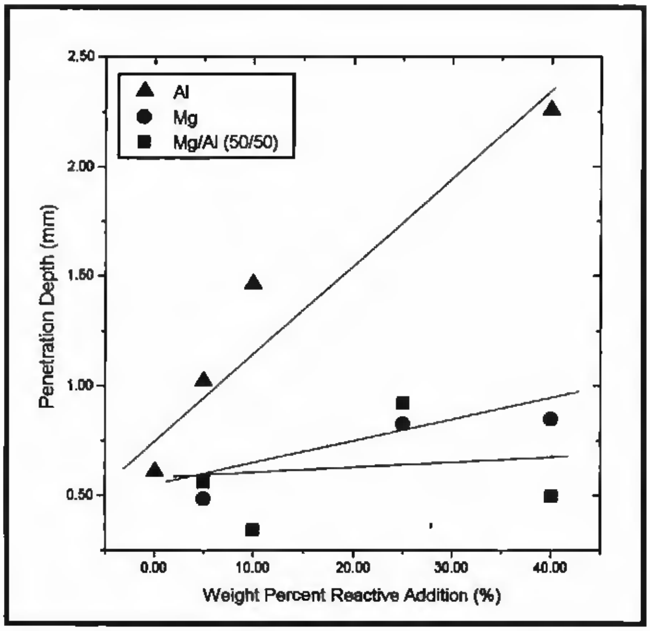

Fig. 7 — Penetration depth as a function of type and amount of reactive addition.

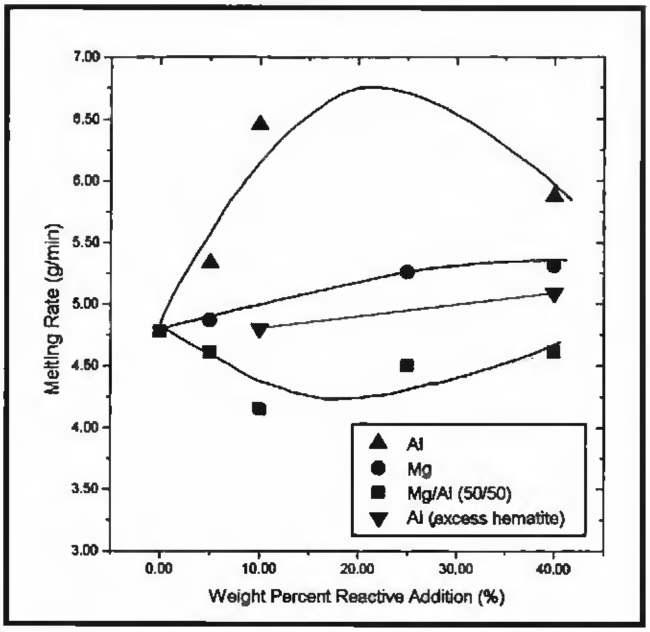

Fig. 8 — The effect of type and amount of reactive addition on electrode melting rate.

plate in the calorimeter and prevent it from touching the dewar walls. The plates were sandblasted, cleaned with acetone and weighed to the nearest 0.1 g immediately prior to welding.

Welding Arrangement and Procedure

A fixture was designed to thermally insulate the base plate to be welded from the work bench. A base plate of predetermined size could be held firmly in place on pins in the fixture by a quick release latch. The latch enabled the specimen to be removed easily and quickly from the fixture and placed into the liquid nitrogen calorimeter.

A Hobart 300-series constant-current transformer-rectifier machine was used to make the welds. The head assembly consisted of an ARCON voltage controller connected to a semiautomatic travel carriage. The voltage controller maintained a set arc length, which helped maintain a constant electrical heat input during welding. Three bead-on-plate welds were made with each electrode formulation. The welding parameters were direct current, reverse polarity, 25 V, 125 A and a travel speed of 2.54 mm/s. One 90-mm weld was deposited on each of the prepared plates and immediately submerged in the liquid nitrogen calorimeter after the arc was extinguished. The amount of time that elapsed between extinguishing the arc and submerging the welded specimen was always less than 5 s. The computer recorded the cooling data, which was analyzed and the necessary information extracted. The welded plates were weighed again to determine the buoyant force and sensible heat of the as-welded plate.

The welded plates were sectioned in the transverse direction, ground, polished and etched. The weld bead cross sections were photographed and measured using the image analyzer. Six 1-g samples were sectioned from the weld metal of each plate. These samples were quantitatively analyzed for oxygen, sulfur, nitrogen and carbon content with a LECO interstitial analyzer.

Results and Discussion

Calorimetric measurement of the as-welded plates indicated that exothermic heating does occur when welding with these electrodes. Visual examination of the arc length indicated that, in all cases, the arc length at the same potential increased as the concentration of exothermic reagent increased. Increasing the arc length tends to broaden the distribution of arc heating and decrease the testing intensity of the arc. Longer arcs also radiate more energy and convect more heat to the atmosphere. Therefore, increases in the arc length with increasing exothermic additions will tend to mask or decrease the actual heating effect. The true exothermic heating potential must be greater than that which is measurable with the equipment used in this research.

Figure 1 shows how calorimetric measurements of heat input change with increasing concentrations of the three types of exothermic reagents. The largest sources of error in the data are probably electrode inhomogeneity and variable power delivered by the welding machine. With all three types of exothermic addition (Mg, Al, Mg/Al), there is a definite trend toward increasing measured heat with increasing concentration of reactive addition.

It is apparent from Fig. 1 that, in all three cases, a maximum measured heat exists in the range of 25–30 wt-% reactive addition. Beyond this maximum, further addition of reagent does not increase the measured heat. This plateau in measured heat indicates that there may be a limit to the amount of reagents that can participate in the exothermic reaction. One limiting factor could be an exhaustion of available oxygen in the region of the reaction. The conditions of welding indicate that the exothermic reaction occurs in a molten metal environment; thus, the solubility limit of iron oxide in iron can limit the amount of oxide available to react.

It is expected that the exothermic reactions occur primarily at the tip of the electrode, significantly affecting the electrode melting rate. Given this assumption, the peak in the measured heat input curve can also potentially be explained by any physical limitations of heat transfer to the molten electrode tip. Limitations can result from chemical heating occurring at locations above the molten tip and by convection losses to the atmosphere. For exothermic additions in excess of 25–30 wt-%, these modes of

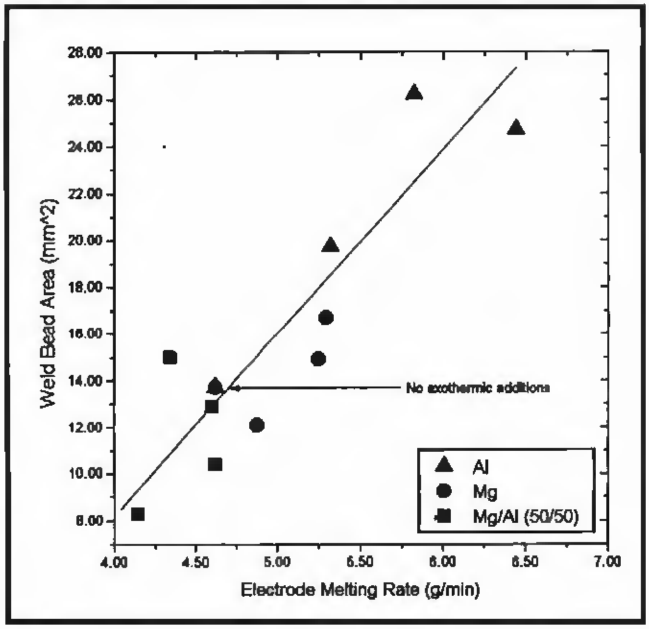

Fig. 9 — Melting rate as a function of weld bead area for the three types of exothermic additions.

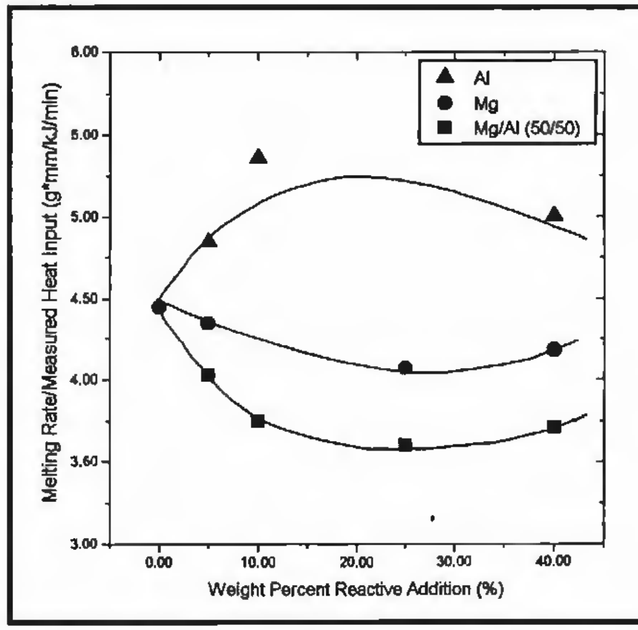

Fig. 10 — Melting rate normalized with respect to measured heat input for the three types of exothermic additions.

heat loss may occur at rates exceeding the rate of heat transfer into the molten tip, resulting in the optimum in the measured heat input curves. The heat that is not lost from the molten electrode tip is transferred to the weldment by the molten droplets.

Figure 1 also illustrates how the measured heat changes with increases in aluminum-reactive addition with excess hematite in the mixture. The curve labeled A was produced from consumables with twice the amount of hematite as the rods that produced curve B. These curves indicate that additional hematite, which is thought to be the primary source of oxygen for the exothermic reaction, does increase the measured heat input. This result confirms that the availability of oxygen influences the heat generated in the exothermic reaction.

To determine the effect of current and voltage on measured heat input, welds were made with the aluminum-reactive series of electrodes at 33 V and 96 A, which gives approximately the same electrical heat input as the previous welds received (1.2 kJ/mm). The measured heat inputs at the two welding parameters for the aluminum-reactive electrodes as a function of increasing reactive addition are shown in Fig. 2. At a current of 96 A and a voltage of 33 V, the measured heat contents are significantly less than those welds produced at 125 A and 25 V. This behavior is seen because higher currents are more efficient at transferring the arc heat and produce larger weld bead and greater penetration than lower currents (Ref. 1). How welding parameters affect exothermic heating cannot be determined from this data. However, Glushchenko (Ref. 15) has shown that the melting efficiency of his exothermic electrodes is optimized at currents in the range of 300–325 A.

Characteristics of the Slags

Slag viscosity and interfacial tensions have been shown to affect weld bead morphology and penetration (Ref. 2). For this reason, it is necessary to review the performance of the slags in at least a qualitative sense before discussing the results of the bead area and penetration study.

In general, the detachability and pore-removing ability of the slags deteriorated as the concentration of exothermic addition increased. It was found that magnesium/aluminum alloy reactive additions up to 10 wt-% produce slags that readily detach during and after cooling and form a relatively symmetric and uniform layer of slag protection. At 25 and 40 wt-% reactive addition, the slag deposit adheres tenaciously to the weld, traps pores in the weld metal and is nonuniform along its length. The shape of the slag deposits were observed to become narrower and taller with increasing amounts of exothermic reagents. Narrow, tall slag deposits tend to be associated with higher viscosity slags.

The slags formed from the aluminum series of reactive consumables demonstrated the best performance. Although the detachability of these slags deteriorated with increasing concentration of reactive addition, no porosity was trapped in the weld metal and the beads were relatively uniform and symmetric along their lengths.

The A series of electrodes (electrode-covering compositions with twice the ratio of hematite to aluminum) produced slags that trapped excessive porosity in the weld metal. Recalling the measured heat data for these welds, which indicated a plateau in the chemical heat production, it seems reasonable that hematite in excess of its solubility in iron would release oxygen in the solidifying weld pool, producing a porous weld bead.

Exothermic Meltback

Once ignited, a purely exothermic reaction can propagate without further addition of energy. Some of the electrodes with 25 and 40 wt-% reactive addition would spontaneously ignite ahead of the arc during welding. With the exothermic reaction outrunning the process of melting the rod, a separation of the energy source from the melting rod tip developed. After the arc was extinguished, the reaction would propagate up the length of the electrode without melting the core wire, very much like a sparkler. These reactions usually were not visible until after 3.5 in. (90 mm) of weld bead was deposited during the calorimetric tests. These premature reactions can seriously limit the applicability of exothermically assisted welding electrodes.

One solution to the premature reaction problem could be to fill a hollow tube with the reactive flux, as in flux cored arc welding. A flux cored rod would better contain the heat generated by the exothermic reaction and may have better electrode melting characteristics. The extra heat imparted to the electrode would then be transferred to the base plate.

Penetration and Weld Nugget Size

The effect of the type and amount of reactive addition on weld bead area is illustrated in Fig. 3. For the aluminum and magnesium additions, the weld bead area increases with increasing concentration of reactive component. For the magnesium/aluminum alloy reactive addition, the weld bead area actually decreases and then increases slightly.

The general trend is toward increasing bead area with increasing concentration of reactive addition. This trend is expected because increasing amounts of reactive addition were found to produce increasing measured heat inputs during the calorimetry tests. The most interesting feature in Fig. 3 is that the aluminum additions produce weld beads approximately twice as large as the magnesium and Mg/Al alloy additions. This difference in weld bead size is interesting because, as Fig. 1 shows, the measured heat inputs change only slightly between the type of reactive element at a given concentration of element. Therefore, there must be other factors influencing weld bead area in addition to the measured heat input.

Figure 1 shows how measured heat input changes with increasing wt-% of reactive addition. The heat inputs produced by the rods with 5 wt-% exothermic addition are boxed to indicate that these rods produced approximately the same measured heat inputs (about 1.1–1.15 kJ/mm). Looking at Fig. 3, it can also be seen that this constant heat input produces weld beads of different area depending upon the type of reactive reagent used in the electrode.

Figures 4 and 5 illustrate that a measured heat input of about 1.2 kJ/mm results in extremely different weld bead sizes depending upon the type of reactive addition used. The points boxed in Fig. 4 correspond to a heat input of approximately 1.2 kJ/mm, which in turn corresponds to the points boxed in Fig. 5. In Fig. 5, equivalent measured heat inputs produced a weld bead area of about 25 mm^2 for the aluminum addition and an area of about 13 mm^2 for the Mg/Al alloy addition. Thus, the type of reactive addition influences how the heat input melts and produces the weld bead.

Figure 6 shows how the weld bead area changes with increasing weight percent of aluminum reactant with and without excess hematite in the mixture. Recall that Fig. 1 indicated that excess hematite, and thus excess oxygen, significantly increased the heat inputs measured with the calorimeter. However, Fig. 6 shows that the weld beads formed with the excess hematite are considerably smaller than those weld beads formed without excess hematite. Once again, it is apparent that heat input is not the primary variable determining weld bead area. This indicates that oxygen may play a role in determining how the weld bead is formed.

Figure 7 illustrates weld penetration depth as a function of the type and amount of reactive addition. The general trend is toward increasing penetration with an increasing amount of reactive addition. Recall that other investigations have shown that penetration and weld bead area increase with increasing current (Refs. 1, 5), and increasing current increases the heat input. Figure 7 shows that the aluminum-reactive component produces considerably deeper penetration than either the magnesium reagent or the magnesium/aluminum reagent. This behavior follows the same pattern as for the weld bead areas and suggests that the type of reactive component influences the penetration.

Electrode Melting

The electrode melting rate plotted as a function of the type and amount of reactive addition is shown in Fig. 8. Figure 9 indicates that melting rate is directly related to weld bead area. For each type of addition (Mg, Al and Mg/Al), the relative magnitudes of melting rate and weld bead area correspond. The direct relationship between weld bead area and electrode melting rate indicates that heat from exothermic reactions causes more electrode to melt per unit time, giving a larger weld bead. Thus, the mechanism influencing the weld bead area and electrode melting rate must be heat transfer by the molten droplets moving from the electrode tip to the base material.

The electrode melting rate produced with no exothermic addition is indicated in Fig. 9. All of the electrodes with additions of the magnesium/aluminum alloy mixture had melting rates below that of the zero exothermic addition rod. The Mg/Al-alloy-rich electrodes also produced the smallest weld beads and had the lowest measured heat input. Thus, depending upon the type of exothermic addition, the electrode melting rate and weld bead size can either increase or decrease.

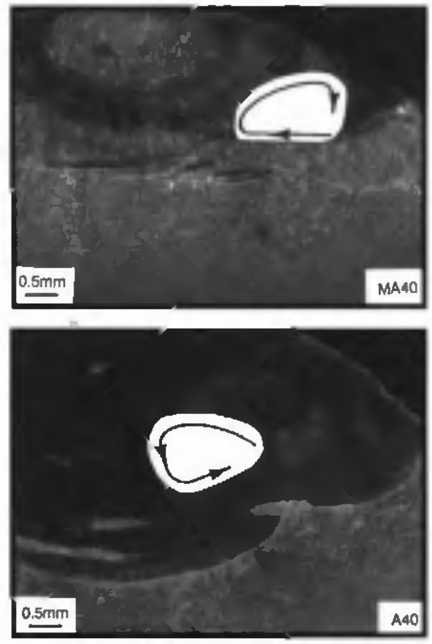

Fig. 11 — Micrographs near the fusion zone indicating stirring patterns.

Electrode melting rates below that produced at the zero exothermic addition level are difficult to explain. The exothermic "meltback" phenomenon could be responsible for decomposing other exothermic components in the flux, causing the very low melting rates of the Mg/Al-alloy-rich rods. Directional weld pool stirring could also promote the smaller weld beads produced with the Mg/Al alloy rods. This suggestion will be discussed further in the weld pool stirring section.

The relationship between the electrode melting rate and the heat inputs measured with the calorimeter for the three types of exothermic additions is shown in Fig. 10. This plot indicates that aluminum additions increase the electrode melting rate more efficiently than either of the magnesium-rich additions. This behavior can be explained by considering the spontaneous reactions observed in the magnesium-rich electrodes. These observations indicate the magnesium exothermic additions are reacting ahead of the welding arc, delocalizing the exothermic source and its heating ability. Thus, it is important to match the rate of the exothermic reactions with the rate at which the arc consumes the electrode. When these rates are equal, the ability of the exothermic reactions to assist in heating and melting is optimized.

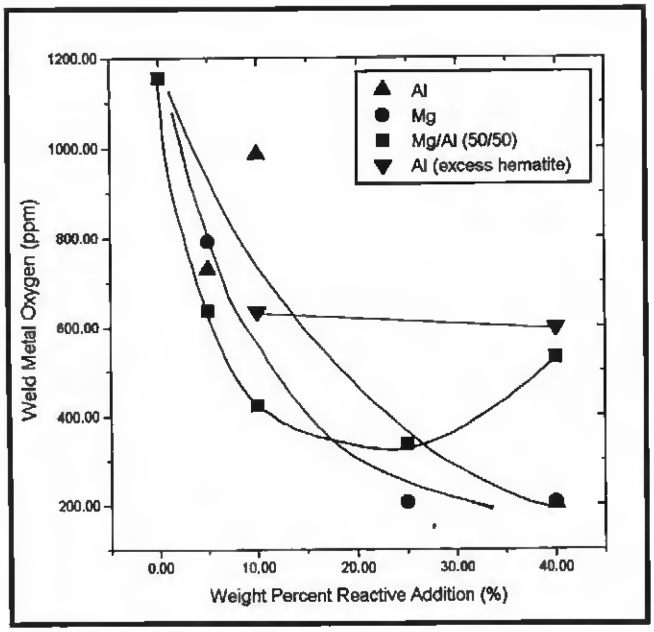

Fig. 12 — The effect of type and amount of reactive addition on weld metal oxygen.

Weld Pool Stirring

It has been shown that minor element additions can influence the stirring patterns in the weld pool and thus affect the weld bead morphology (Ref. 22). Although these studies used the GTAW process, the results presented here suggest that weld pool stirring may play a part in the SMAW process as well.

Two primary factors contribute to weld pool stirring. Current flowing into the weld pool exerts a force (Lorentz force) on the liquid metal, which will circulate the molten metal downward at the center and radially outward at the bottom of the pool. This pattern of metal flow enhances the flow of heat and tends to produce a relatively deep weld pool (Ref. 22). The second force originates from surface tension gradients (Marangoni effect) produced by temperature gradients at the weld pool surface. Near the center of the weld pool, the arc heating is greater than the weld pool edge, which is solidifying. Depending upon the weld pool composition, this temperature gradient can produce a positive or negative surface tension gradient, which influences surface metal flow (Ref. 20). Low concentrations (less than 150 ppm) of surface-active elements (S, O and Se) have been found to substantially alter the shape of GTA weld deposits. In the presence of surface-active elements, the surface tension temperature coefficient is positive, producing a relatively deep and narrow bead geometry. With low concentrations of surface-active elements, the surface tension temperature coefficient is negative, producing a wide pool with shallow penetration.

The dominant pool stirring mode has been shown to be related to the magnitude of the welding current. Below approximately 150 A, pool stirring is dominated by the surface tension gradient. Above 150 A, pool stirring is dominated by the Lorentz force.

Metallographic observation of the weld beads revealed evidence of stirring patterns. Figure 11 shows micrographs taken near the weld interface of the welds from two different types of exothermic-assisted electrodes. Two distinct patterns are evident in the welds. The weld made with the A40 electrode (aluminum addition) shows patterns consistent with negative convective flow, *i.e.*, metal moving downward from the top centerline toward the root of the weld. The welds made with the MA40 (magnesium-aluminum combination) electrode show evidence of positive convective flow, *i.e.*, metal moving radially outward from the centerline.

Two features present in the weld beads indicate the type of stirring: the overall shape of the weld bead and the shape and orientation of the undercut base plate near the weld interface. Negative string tends to form deep, narrow weld beads, like that of the A40 weld bead. Positive stirring forms shallow, wide weld pools, like the M40 and MA40 weld beads. Negative stirring, directed downward toward the root of the weld bead and then up along the edges of the pool, tends to undercut the base plate near the weld interface (mushy zone), forming the wave-like structures present in the A40 weld bead. Positive flow tends to undercut in the opposite fashion, producing an uplifted base plate such as is present in the M40 weld bead.

Magnesium additions of 3 and 6 wt-% to the flux coating of SMAW electrodes has been shown to produce very low weld metal oxygen and sulfur contents. Magnesium and magnesium/aluminum alloy additions clean the weld pool of sulfur more effectively than the aluminum-reactive additions. This cleaning would explain the differences in size and shape of the weld beads formed under the action of the three types of fluxes.

At currents less than approximately 150 A, weld pool stirring is controlled by the surface tension gradient, which is in turn influenced by weld metal sulfur and oxygen (Ref. 22). Chemical heat generation during exothermic welding is controlled by the reaction of a metal with oxygen. Thus, a measure of the weld metal oxygen should, in some fashion, reflect the measured heat input, weld bead area and penetration depth. Figure 12 shows weld metal oxygen content as a function of the type and amount of reactive addition. For each type of reactive addition, weld metal oxygen content decreases with increasing weight-percent reactive component. Recalling the measured heat input curves in Fig. 1, it is apparent that they are reciprocal of the data shown in Fig. 12. This correspondence indicates that the plateau in heat input may be due to the exhaustion of available oxygen to react. Additionally, excess hematite (the reaction oxygen source) produced the greatest measured heat input and a stable weld pool oxygen content. This result suggests a saturation point at which the size of the molten droplet controls the amount of reactive addition (metal plus oxide) that can react. The level of weld metal oxygen can become very low and may approach the transition value for negative to positive stirring.

Summary

Calorimetric measurements of heat input indicate that exothermic mixtures of magnesium, aluminum and magnesium/aluminum alloy plus hematite can assist in heat generation during shielded metal arc welding. Increases in heat input up to approximately 25 to 30% of the heat required to weld were attributed to chemical heat generation. There appears to be slight differences in the quantity of heat generated by different reactive components. The supply of oxygen to the reaction limits heat generation.

The melting rate data clearly indicate that the exothermic reactions occur at the molten electrode tip. The heat from these reactions increases the melting rate of the electrode and is transferred to the plate in the molten droplets. The aluminum exothermic reactions occur at a rate that allows the resulting heat to be incorporated into the electrode droplet, giving higher electrode melting rates and more base-plate heating than the magnesium exothermic reactions. The magnesium exothermic reactions occur before the arc melts the droplet, and so the excess heat is not incorporated into the droplet, but is instead lost to the atmosphere or used to accelerate the reaction of the exothermic components higher up in the electrode coating.

Increasing concentrations of exothermic mixtures in the coating of SMAW consumables increase measured heat input, weld nugget area, weld penetration depth and electrode melting rate and decrease weld metal oxygen content. Weld bead area and penetration measurements correlate very well with the melting rate data. The higher melting rate obtained with the aluminum additions produced larger weld bead areas and greater penetration depth. Weld metal sulfur and oxygen content, through their effect on weld pool stirring, may play a role in determining the melting characteristics of the weld bead.

Conclusions

1) Exothermic reactions can assist in the production of heat during shielded metal arc welding.

2) It is essential to control the oxygen content to achieve both optimized chemical and physical responses when developing exothermic welding consumables.

3) Weld deposition is enhanced more with aluminum-reactive additions, producing a greater electrode melting rate and a larger weld bead, than with magnesium-rich additions.

4) The exothermic reactions need to occur predominantly at the tip of the electrode, with the chemically generated heat being transferred to the weld pool by the transfer of molten metal droplets.

Acknowledgment

The authors acknowledge and appreciate the support of the U.S. Army Research Office.

References

1. Jackson, C. E., and Shrubsall, A. E. 1953. Control of penetration and melting ratio with welding technique. *Welding Journal*, 32(4): 172-s to 178-s.

2. Schwemmer, D. D., Olson, D. L., and Williamson, D. L. 1979. The relationship of weld penetration to the welding flux. *Welding Journal*, 58(5): 153-s to 160-s.

3. Natalie, C. A., Olson, D. L., and Blander, M. 1986. Physical and chemical behavior of welding fluxes. *Material Science Annual Review*, Vol. 16, pp. 389–413.

4. *Welding Handbook*, 7th Ed., Vol. 1. 1981. American Welding Society, Miami, Fla. p. 37.

5. Jackson, C. E. 1959. The science of arc welding. *Welding Journal*, 38(5): 177-s to 119-s.

6. Chandel, R. S. 1990. Electrode and plate melting efficiencies of submerged arc welding and gas metal arc welding. *Materials Science and Technology*, 6(9): 772–777.

7. Chandel, R. S. 1987. Mathematical modeling of melting rates for submerged arc welding. *Welding Journal*, 66(5): 135-s to 140-s.

8. Robinson, M. 1961. Observations on electrode melting rates during submerged arc welding. *Welding Journal*, 40(10): 503-s to 515-s.

9. Niles, R. W., and Jackson, C. E. 1975. Weld thermal efficiency of the GTAW process. *Welding Journal* 54(1): 25-s to 32-s.

10. Lesnewich, A. 1958. Control of melting rate and metal transfer in gas-shielded metal arc welding. *Welding Journal* 37(9): 343-s to 353-s.

11. Wilson, J. L., Claussen, G. E., and Jackson, C. E. 1956. The effect of I^2R heating on electrode melting rate. *Welding Journal*, 35(1): 1-s to 8-s.

12. Hummitzch, W. 1948. New facts on electric-arc reactions of coated welding electrodes. *Schweisstechnik*, 2, 50–54, May; 67–70, June; 84–89, July.

13. Underwater cutting process surfaces for new applications. 1989. *Welding Journal*, 68(7): 59–60.

14. Chase, M. W., Davies, C. A., Downey, J. R., Frurip, D. J., McDonald, R. A., and Syverud, A. N. 1985. JANAF thermodynamic tables. *Journal of Physical and Chemical Reference Data*, 3rd Ed., Vol. 14.

15. Glushchenko, A. S. 1980. Determination of the productivity of the thermit arc welding process under an exothermic flux. *Svar. Proiz.*, 37–39, September.

16. Zarechenskii, A. V. 1982. Increasing the efficiency of flux cored strip melting. *Svar. Proiz*, 38–39, July.

17. Karpenko, V. M. 1980. The melting parameters of welding electrodes with an exothermic coating mixture. *Svar. Proiz*, 33–37, September.

18. Ioffe, O. M. 1980. The effect of the titanothermite mixture in the electrode coating on the increase in the productivity of welding. *Svar. Proiz*, 29–32, March.

19. Flemming, D. A., Bracarense, A., Lui, S., and Olson, D. L. 1996. Toward developing a SMA welding electrode for HSLA-100 grade steel. *Welding Journal*, 75(6): 171-s to 183-s.

20. Watkins, A. 1989. Heat Transfer Efficiency in Gas Metal Arc Welding. Master's thesis, University of Idaho, Moscow, Idaho.

21. Hoffmann, R. L. 1979. Mild steel electrode coverings — How they work. *Welding Journal*, 57(5): 408–410.

22. Burghardt, P., and Campbell, R. 1992. Chemistry effects on stainless steel weld penetration. *Key Engineering Materials*, 69 and 70, p. 379, Transactions of Technical Publications, Switzerland.